JOURNAL OF MATERIALS SCIENCE **34** (1999) 5113–5126

Studies of microstructural and mechanical properties of Nylon/Glass composite

Part II *The effect of microstructures on mechanical and interfacial properties*

HELEN C. Y. CARTLEDGE
Centre for Advanced Materials Technology, Department of Mechanical and Mechatronic Engineering, University of Sydney, NSW 2006, Australia
E-mail: helen.cartledge@dsto.defence.gov.au

CAROLINE A. BAILLIE*
Department of Materials, Imperial College of Science, Technology and Medicine, Prince Consort Road, London SW7 2BP, UK

This is a part of a series of studies on the influence of thermal processing on microstructures and mechanical properties of thermoplastic composites. In this paper, the effect of cooling rate during thermal moulding processes on the mechanical properties of bulk unidirectional commingled yarn GF/PA6 composites (Iosipescu shear strength, transverse flexural tensile strength and elastic modulus) has been investigated. Cooling rate from fast to slow, $-60\,^{\circ}$C/min, $-3\,^{\circ}$C/min and $-1\,^{\circ}$C/min, were achieved at 1.5 MPa pressure. Scanning electron microscopy (SEM) was used to analyse the damaging mechanisms of the fracture surfaces of the tested samples. The different dynamic responses of the samples were observed by polarised optical microscopy (POM) during the mechanical tests. The results indicated that when the cooling rate was varied from fast to slow, the interfacial tensile and shear strength were improved associated with enhanced elastic modulus. These results may be attributed to the slow cooling achieved a high transcrystallinity between the glass fibres and PA6 matrix, and high crystallinity of α phase in the PA6 matrix.

1. Introduction

The mechanical properties of fibre-reinforced polymer composites is primarily dependent upon the following three factors: (1) strength and modulus of the fibre, (2) strength and modulus of the matrix, and (3) effectiveness of the bond between fibre and matrix in transferring stress across the interface [1, 2]. These factors are basically determined by the microstructural details of these materials which include transcrystallinity of the interface, crystallinity and spherulite size of the matrix which are in turn controlled by thermal processing of these materials [3].

The interface between the fibres and the matrix in the composite materials is widely regarded as the most important factor determining their mechanical properties [2, 4–7, 8–11]. In addition transcrystallinity has a significant effect on various mechanical properties [12]. However, as yet few measurements of such effects on bulk composite samples have been conducted, and it is still debatable as to whether transcrystallinity increases or decreases the interfacial strength, consequently affecting the performance of thermoplastic composite materials. Moreover, the nature of the crystalline phase affecting the mechanical properties of these materials has never been systematically investigated.

In this series of studies, it was found that a large diameter transcrystalline layer existed between the glass fibres and the PA6 matrix of the slow cooled GF/PA6 samples as well as high crystallinity of PA6 α phase. The effect of thermal processing on microstructures of matrix and interfaces, is presented in the part 1 of this paper [13]. In this part of the paper, the effect of cooling rate during thermal processing on the mechanical properties and interfacial bonding strength of the thermoplastic composites in relation to the transcrystallinity and crystallinity of these materials will be explored.

Selection of the methods for measuring the interfacial strength is still a very controversial topic in composite interfacial studies. For instance, the short beam shear test, the transverse tensile test, the transverse flexural test and the Iosipescu shear test can be used to measure the interfacial bond of bulk composites. However, the failure mode during the testing can be very complex, and therefore, none of these tests could really be

*Author to whom all correspondence should be addressed.

described as a simple and reliable test, or appropriate for the determination of the interfacial bonding strength for all fibre composites. Further, the test results can be difficult to interpret since failure during the test may not be due to debonding (adhesive failure) in the interfacial layer, i.e., separation may not occur between the fibre and matrix. Rather, it could occur within a fibre, or within the matrix (cohesive failure).

However, from a practical point of view, it may not matter whether the failure during testing is adhesive or cohesive, as long as the strength of the weak link at the interface is being measured. Thus, the most important issue is that the test result can be used to indicate the stress transferred through the interface, regardless of the failure mode. Furthermore, SEM photos may be useful for helping to determine the failure mode and interpret the failure mechanisms.

In this paper, in order to study the influence of transcrystallinity and crystallinity on the mechanical properties and interfacial bond strength of the GF/PA6 composites, the transverse flexure and longitudinal Iosipescu tests were adopted to test the bulk GF/PA6 composites subjected to the different cooling processes.

The transverse flexural test (three point bend), has only recently been used for interfacial bond studies. This is the simplest and the most widely used test for the determination of interfacial bond strength [14–18]. In this test, the fibres are oriented perpendicular to the load direction. Thus the failure can be controlled by the matrix or the fibre/matrix bond. This method, however, is a sensitive test for assessing the interfacial bonding condition. It can be very sensitive to internal defects such as voids or crossed fibres and it should be considered as a "weakest link" test.

The Iosipescu shear test method was originally proposed by Iosipescu in the early 1960s [19]. In 1967 [20], Iosipescu published a detailed study involving the development of the asymmetrically loaded notched beam test to measure the shear strength of isotropic materials (metals). The Iosipescu test method was first applied to composite materials by Thomas Place in the early 1970s [21]. In this test, double-V-notch specimens were employed. The principle of this shear test was that a constant shear force was induced through the mid-length of the specimen, thus producing a pure shear loading at that location (see Fig. 1). A state of pure shear stress was achieved between the two V-notches at the mid-length of the specimen through the action of load couples which produce counteracting moments.

In practice, however, some non-uniformity of the shear stress distribution in the test section occurs, probably arising from small normal compressive stresses. It is possible to prevent specimens failing in the compression by changing the geometry of the specimens compared with that specified in ASTM D5379/D5379M-93 which cannot be applied to all composites.

2. Specimen preparation

2.1. Materials system

The unidirectional commingled yarn GF/PA6 was supplied by Toyobo Co. Ltd., Japan. The original data of the GF/PA6 commingled yarn system which were given by the manufacturer were that the E-glass fibre weight fraction W_f was 60% and density of the GF/PA6 was 1.7 g/cm^3.

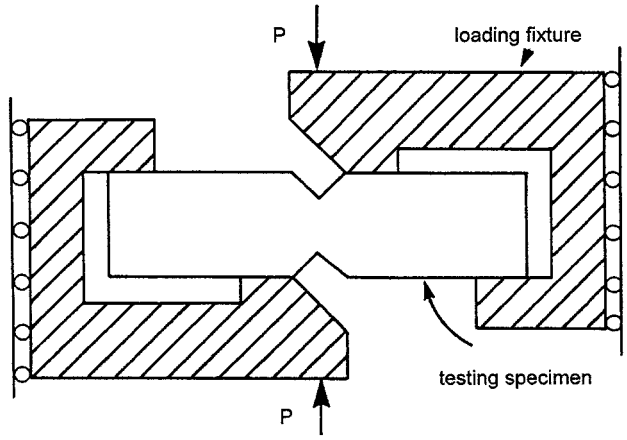

Figure 1 Diagram of Iosipescu test for 0 degree GF/PA6 composite specimen.

2.2. Manufacture processes

The GF/PA6 commingled yarn was wound unidirectionally onto the steel plate at 40 rev/min giving 15 yarn per inch in the winding machine. The yarn was welded together along a line 10 mm away from the edge of the steel plate on both sides with a 40 w soldering iron. The GF/PA6 sheets were cut off from the steel plate along the edge. Fourteen commingled yarn sheets were laid up unidirectionally in the mould. To prevent the PA6 sticking on the mould during consolation, a surface free energy of GF/PTFE cover sheet (CHEMGLAS) was inserted between the GF/PA6 composites and steel mould. The consolidation process was carried out on a hydraulic hot-press machine, Moore G748. The first stage of heating the sample above the PA6 melting temperature took approximately 10 min and pressure were applied on the top and bottom platens of the hot press machine. Once the sample reached 240 °C, the pressure was constantly kept at 1.5 MPa to squeeze out air and excess resin sealed the mould prevented oxidation degradation of the PA6. The moulding temperature was from 235 to 240 °C and the holding time was 10 min with constant pressure through out the whole process.

To obtain the different microstructures in the composites, the moulds were cooled down at three different rates in the hydraulic press machine under 1.5 MPa pressure. A thermal measurement unit was used to record and monitor the temperature changing during the whole consolidation process. The cooling rate of the consolidation processes was recorded as follows:

1) −1 °C/min, cooled down in the hot-press;
2) −3 °C/min, cooled down with air circulated through the plates of the hot-press machine;
3) −60 °C/min, cooled down with cold water circulated through the plates of the hot-press machine.

Fig. 2 shows the thermal history of the GF/PA6 composite consolidation. The final sample was of dimension

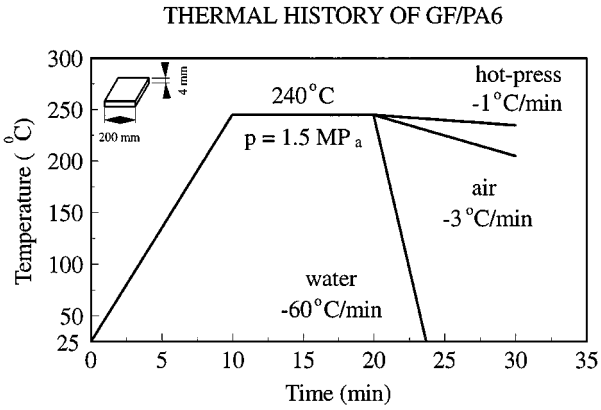

Figure 2 Thermal histories of GF/PA6 composite samples.

$200 \times 200 \times 4$ mm and it was a white colour implying there was no oxidising degradation during the thermal processing.

2.3. Transverse flexural testing specimens

Nine transverse flexural testing specimens for each cooling condition were prepared. The specimens were cut off from the three differently cooled unidirectional GF/PA6 bulk samples by an electrical band saw at speed 550 m/min with air cooling to avoid the cutting heat affecting the microstructures of the GF/PA6 samples. The geometry of the specimens were $10 \times 80 \times 4$ mm and with the fibres perpendicular to the specimen length. The cutting edge of the specimens was polished in the lengthwise direction of the specimen with P600 emery paper.

2.4. Iosipescu intralaminar specimen

Eight Iosipescu intralaminar specimens for each cooling condition were prepared. The specimens were cut with fibres parallel to the longitudinal axis-0 degree from GF/PA6 composite. The specimens were 80 mm long, 20 mm wide and 4 mm thick. Two 90° angle notches were cut at the specimen midlength with faces oriented at $+45^\circ$ and -45° to the longitudinal axis. The notches were introduced using a vertical milling machine Pacific FTV-2S with a specially designed parallel fixture. Special care was taken to use optimum cutting rates. A freshly-sharpened cutting tool was used to minimise pre-test damage and produce a sharp notch. The notch tip radius was about 120 μm. The width between the two notches' tips was selected as 3 mm for the optimum value to achieve a pure shear failure in the midspan section of the specimen during the test. The optimum processing of the specimen cutting and failure modes investigation are discussed in a separate paper by the authors.

3. Experimental technique

3.1. Transverse flexural test

The 90° three point flexural tests were performed at room temperature on an Instron 4302 table-top load frame in compression according to ASTM standard

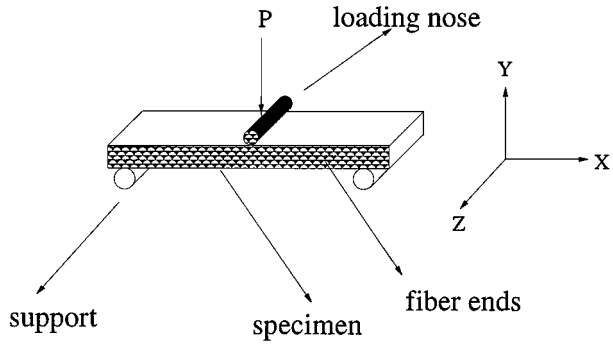

Figure 3 Transverse flexural test of GF/PA6 bulk composite sample.

D790M-92. The tests studied the influence of the cooling rate during the thermal process on the GF/PA6 composite interfacial bonding condition. As Fig. 3 illustrates, the specimen was loaded along the fibre orientation with loading speed 1.7 mm/min. The supports span was 64 mm and the support span to the depth ratio was 16 : 1. Radius of the supports and loading nose was 5 mm. A 1 kN load cell was used to collect the signal of the load and displacement in the test and then electronically logged on a computer. A microscope was used to observe the dynamic fracturing process during the tests.

Maximum tensile stress. At a given load P, the maximum pure bending tensile stress σ_b, which was parallel to the specimen length, lay along a line on the surface below the centre loading point and is given by

$$\sigma_b = \frac{3PL}{2bd^2}$$

where σ_b is the maximum bending tensile stress at the midspan of the specimens (MPa), P is peak load at rupture (N), L is support span (mm), b is width of the beam specimens (mm), and d is the thickness of the beam specimens (mm).

Using this testing arrangement enables the tensile strength of the interface to be evaluated by substitution of the failure load or peak load into the above equation.

Elastic modulus. The elastic modulus of the GF/PA6 composites can be calculated by drawing a tangent to the steepest initial straight-line portion of the load-deflection curve and using the following equation

$$E_b = \frac{L^3 m}{4bd^3}$$

where E_b is the modulus of elasticity (GPa), L is support span (mm), m is slope of the tangent to the initial straight line portion of the load-deflection curve (N/mm), b is width of the beam specimens (mm), and d is the thickness of the beam specimens (mm).

The standard deviation of the strength and elastic modulus was calculated as follows

$$s = \sqrt{\frac{\Sigma y^2 - n\bar{y}^2}{n-1}}$$

where s is the estimated standard deviation, y is value of single test, n is number of tests, and $\bar{y}$ is the arithmetic mean of the set of tests.

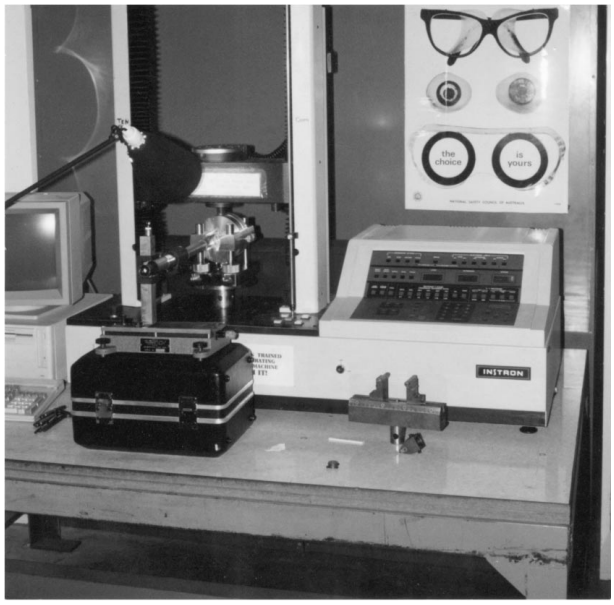

Figure 4 Optical microscopy observation of dynamic response of Iosipescu test.

3.2. Iosipescu intralaminar shear test

The eight 0° Iosipescu specimens for each cooling condition were tested at a constant cross-head displacement rate of 2 mm/min according to ASTM D5379/D5379M-93 and were carried out on an Instron 4302 machine at room temperature. A 10 kN load cell was used to collect the signal of the load and displacement in the test and then logged to a computer to be processed.

The test fixture was based on the original Wyoming University test fixture developed by Walrath and Adams, and made by this research centre. Iosipescu tests in this study were performed under monotonously applied compressive loads normal to the longitudinal axis of the specimen (axis of the fibres). The mechanical dynamic response of the tests were observed by a microscope as shown in Fig. 4.

A state of pure shear was achieved within the midspan section of the Iosipescu test specimen by applying two counteracting moments which were produced by two force couples-P. From the simple statics considerations, the shear force acting at the centre of the cross section was equal to the applied force as measured from the load cell. There was no stress concentration at the sides of the notches, because the normal stresses were parallel to the sides at that point of the specimen. Consequently, the shear stress was obtained by simply dividing the applied force by the net cross-sectional area between the two notch tips. The shear stress can be calculated as

$$\tau_i = P/A$$

where τ_i is the shear stress at ith data point (MPa), P is load at ith data point (N), $A = Ld$, cross-sectional area (mm^2), t is the width between the two tips of the notch (mm), and d is the thickness of the beam specimen (mm).

3.3. Electron microscopic study

The fractured surfaces were examined using a Scanning Electronic Microscope. The specimens were sputter coated with a thin layer of gold in order to improve the resolution of the specimen prior to SEM examination. For the low resolution of the GF/PA6 an accelerating voltage was selected at 20 kV and the condenser lens (spot size) was selected as 100 nm. Both backscatter and secondary electron detectors were used.

4. Microscopy observation of dynamic response

4.1. Transverse flexural test

During the flexural tests a microscope was used to observe the dynamic response of the specimens under a compressive load. It was seen that when the loading force reached the peak value, fracture starts from the bottom of the specimens at the midspan and spreads along the y-axis. It occurred as mode I fracture behaviour in the damage zone.

It was found only one crack appeared in the air (CII) and water (CIII) cooled samples, but the length of the crack was found to be longer for the latter. In the hot-press cooled sample, CI, two cracks were observed, a small crack accompanying with a long crack. It was observed with the microscope that many small cracks appeared on the top side of the CI specimen. The small cracks absorbed the energy from the compressive load in the bending test in the CI specimens.

The initial crack length at the peak load was found to be proportional to the cooling rate of the specimen. Increasing cooling rate led to increasing the initial crack length and reducing peak load as listed in Table I. Table I shows the effect of cooling rate on the initial crack length and beam deflection at peak load or break.

Therefore, it appears that the initial crack length reflected the interfacial bonding condition. The slow cooling process resulted in a columnar crystalline structure growth along the glass fibres as presented in the part 1 of this paper by the authors [13], may give the GF/PA6 composite a strong interfacial bond. Then the strong interfacial bond stopped the crack spreading further.

The peak loads at fracture for the air and water cooled samples were very close to each other as Figs. 5 and 6 show. It probably because they have very similar interfacial bond conditions as shown in the part 1 of this paper by the authors [13], a slight difference in the crystallinity and approximately equal γ phase volume contents as listed in the Table II. The γ phase appears as a lower density and lower strength amorphous material. Damaging an equal volume of the α and γ crystalline matrix, the α phase material may require extra energy compared with the γ phase.

TABLE I Effect of cooling rate on initial crack length and beam deflection at peak load

Sample cool rate (°C/min)	Peak load at break (N)	Cracking length (mm)	Beam deflection (mm)
CI: −1	71.5	1.2	2.0
CII: −3	57.58	1.6	1.77
CIII: −60	56	2.0	3.0

TABLE II The XRD results of PA6 crystallinity and peak area of intensity in GF/PA6 composites

Samples' cooling rate (°C/min)	($\alpha + \gamma$) Peak area	Crystallinity PA6 (%)
CI: −1 (hot-press)	$127 + 4.72 = 131.72$	37
CII: −3 (air)	$52.94 + 20.62 = 73.56$	20
CIII: −60 (water)	$33.61 + 27.19 = 60.8$	17

Another point to be noted in the Table I and Fig. 6, was that the beam deflection at break, water cooled sample CIII, was 3 mm, highest of the three different cooling samples. It is attributed to the lowest crystallinity and highest amorphous content. A high amorphous component gives the materials a visco-elastic nature appearing rubbery with high elongation.

4.2. Iosipescu intralaminar test

The dynamic response of the 0° oriented specimens was initially linear as shown in Fig. 7. The on-set of non-linear behaviour occurred at approximately 0.7 kN for the hot-press cooled sample, 0.6 kN for the air cooled sample and 0.45 kN for the water cooled sample, respectively.

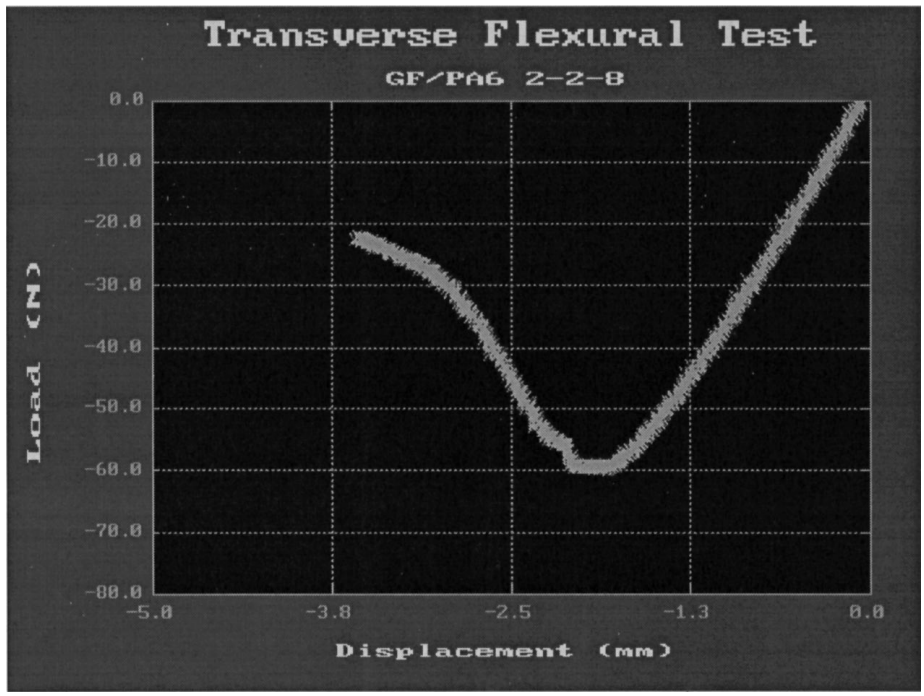

Figure 5 Load-displacement curve of air cooled GF/PA6 in 90° flexural test.

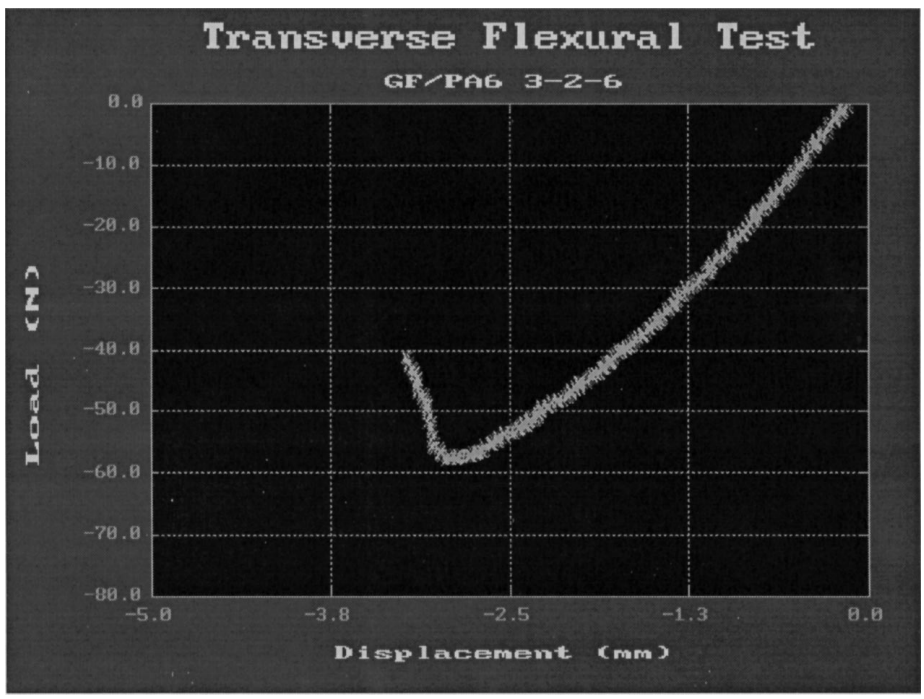

Figure 6 Load-displacement curve of water cooled GF/PA6 in 90° flexural test.

TABLE III Cooling rate effect on the dynamic response of GF/PA6 specimens

Samples (°C/min)	Nonlinear start (kN)	First axial split (kN)	Secondary fail (kN)	Ultimate fail (kN)
CI: −1	0.7	0.8	1.1	1.45
CII: −3	0.6	0.7	0.9	1.1
CIII:−60	0.45	0.6	0.8	0.95

First axial splitting under the notches (at the tips) were observed, manifested by a load drop appearing on the load-displacement curves. The load drop was 0.8 kN for the hot-press cooled samples, 0.7 kN for the air cooled and 0.6 kN for the water cooled samples, respectively, as shown in Table III.

The axial crack tended to initiate at the notch root and propagate parallel to the axis on one side of the notch tip and opposite to the loading points (see Fig. 8). The crack growth in the principal stress plane 45° to the axis were prevented by the axially aligned fibres. The shear stress concentrating at the notch tips were primarily responsible for the cracking initiation. These cracks relieved the local stress concentrations at the notch tips.

The actual stresses associated with the initiation and propagation of the cracks in the tips area were complex. At the first stage, the initial crack propagation was primarily associated with mode I fracture. As the crack extended, the mode II contribution to the fracture increased. These cracks were stopped as they propagated into low stress regions.

Subsequently, few cracks along the fibre orientation appeared between the notch tips in the specimen mid-section. The load drops again significantly which was termed secondary failure in the test. The cracks consisted of numerous short interfacial cracks. They were manifested in the SEM photos and will be discussed in the next section. The cracks propagated in both directions along the fibres and finally caused the specimen to the ultimately fail.

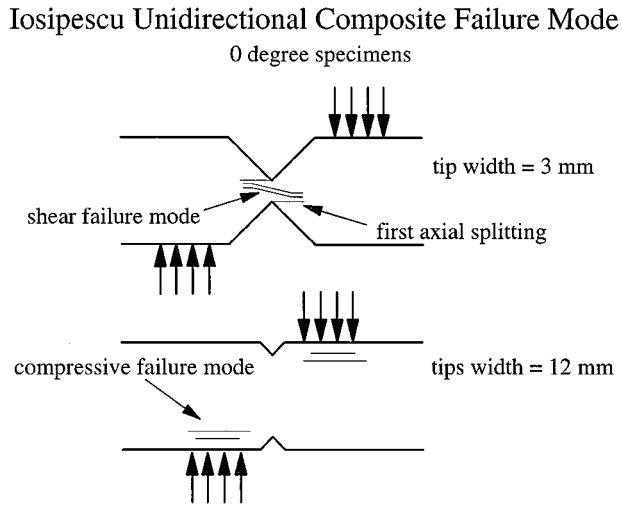

Figure 8 Illustration of Iosipescu test failure modes with different tips width.

5. Experimental observation and discussion

5.1. Mechanical properties

5.1.1. Transverse flexural properties

The results of the flexural test showed that the slowest cooled sample has the greatest flexural tensile strength at the midspan of the specimens where the state of the stress was pure tensile stress. Increasing cooling rate reduced the strength. The relationships between cooling rate and maximum stress occurring at the lowest point of the specimens are shown in the Table IV. The results also showed the effect of the cooling rate on the 90° elastic modulus. Decreasing cooling rate led to enhanced elastic modulus as the Table IV shows.

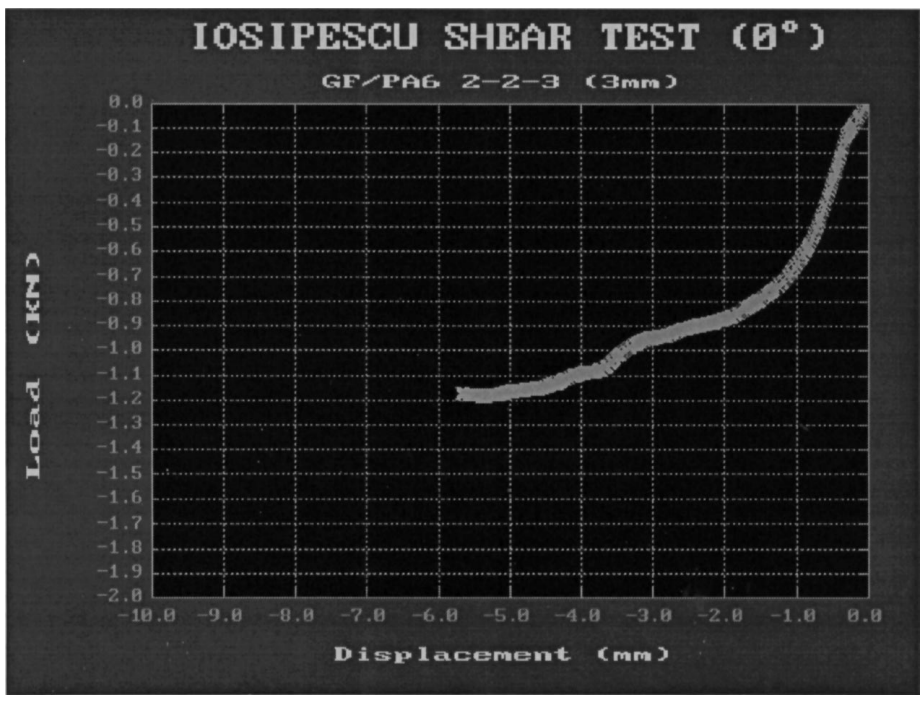

Figure 7 Load-displacement curve of air cooled 0° specimen in Iosipescu test.

TABLE IV Transverse flexural stresses and elastic modulus of GF/PA6 cooled in different cooling rate

Sample's cooling rates (°C/min)	Max σ_b (MPa)	Modulus E_b (GPa)
CI: −1 (hot-press)	43	4.3
CII: −3 (air)	34.5	3.5
CIII: −60 (water)	33	2.4

TABLE V Cooling rate effect on shear strength at failure points

Samples (°C/min)	Secondary shear fail strength (MPa)	Ultimate shear fail strength (MPa)
CI: −1 (hot-press)	91.7	120
CII: −3 (air)	75	91
CIII: −60 (water)	66.7	79

The high tensile strength obtained in the transverse flexural test may be attributed to the good interfacial bond of the GF/PA6 composites which was achieved in the slow cooling process. The high crystallinity of the matrix, and the high ratio of α and γ phases may have contributed to the high flexural strength as well. The high crystallinity of α phase also gave the matrix high density which led to high stiffness and hardness.

The transverse flexural tensile strength obtained from this three-point bend tests has been found to depend on the volume fraction of fibres by some authors [22]. However the failure may not be a adhesive failure between the fibre and matrix. The failure may take place close to the interface but in the fibre or in the matrix which is a cohesive failure. As a result the flexural tensile strength cannot be considered as true values for the interfacial bond strength. Therefore, without a micro-analysis of the ruptured surfaces, it can not be determined whether the tensile strength related to the interfacial tensile strength. If the rupture occurred between the fibre and matrix, the tensile strength can be used to indicate the interfacial tensile strength. Otherwise, if the rupture occurred in the matrix region the tensile strength only represented the matrix properties. In Section 5.2.1, the micro-analysis of the ruptured surfaces or fracture surfaces of the GF/PA6 will be discussed in detail by using SEM techniques.

5.1.2. Iosipescu intralaminar properties

During the Iosipescu tests, it has been observed that the nonlinear/yield point started from 0.45 to 0.7 kN for the three different cooled samples as Table III lists. Reducing cooling rate led to an increase yield point load in the load-displacement curve. This may be attributed to the fact that slow cooling gave the samples high crystallinity and high ratio of α/γ phases resulted in high density and stiffness in the GF/PA6 composites. The slow cooling rate also gave the samples higher axial splitting load, secondary and ultimate failure load than the fast cooling processes. This may be attributed to the strong interfacial bond of the GF/PA6 composites.

The Iosipescu test results indicated that the shear strength was significantly affected by the cooling rates during the manufacturing of the GF/PA6. The slow cooling rates gave the specimens higher axial splitting tensile strength, secondary shear failure strength and ultimate shear failure strength than the faster cooling processes (see Table V).

In the next section, SEM photos will tell us whether the failure occurred in the interface. However, the information obtained (strength of the weak link) from the Iosipescu test still can give us a general idea about the effect of the cooling rate on the mechanical and interfacial bonding conditions of the GF/PA6 composites.

5.2. SEM study of fracture surfaces

5.2.1. Transverse flexural fracture surfaces

The effect of the cooling rate on the interfacial bond can be seen in Figs 9–11 which are the flexural transverse fracture surfaces of the three different cooling rate specimens. Clearer fibre surfaces with less fibre breakages appeared in the Figs 10 and 11 which were the

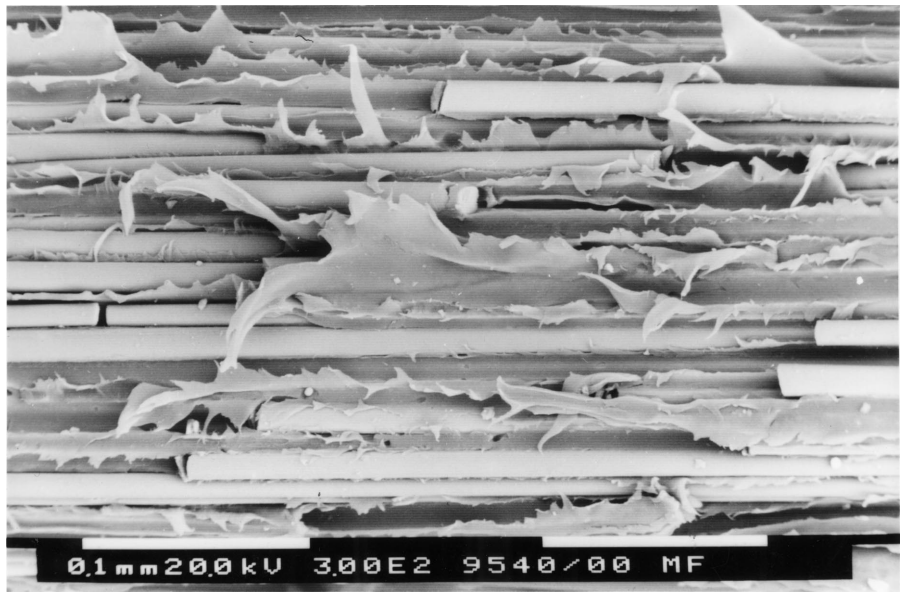

Figure 9 SEM photo of fracture surface of flexural test of hot-press cooled sample.

Figure 10 SEM photo of fracture surface of flexural test of air cooled sample.

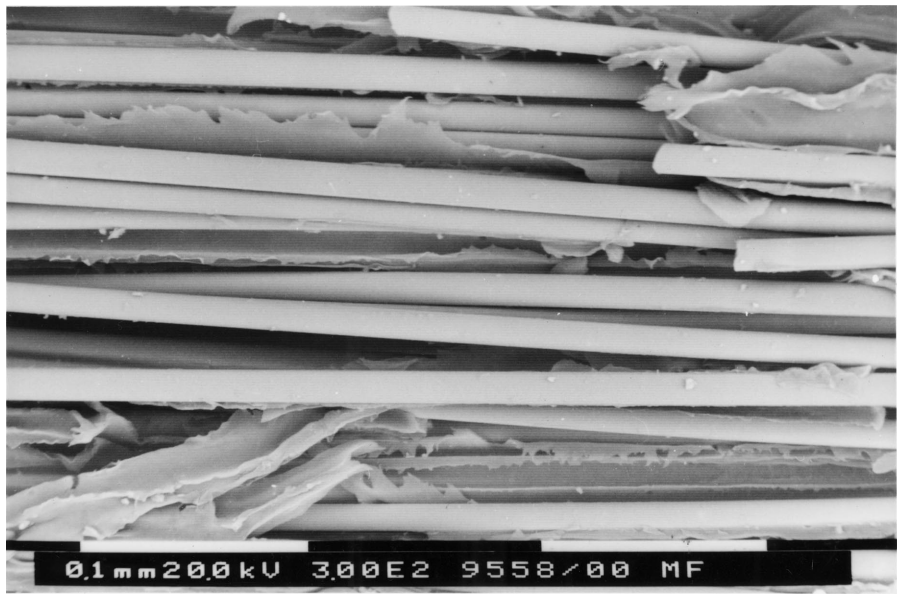

Figure 11 SEM photo of fracture surface of flexural test of water cooled sample.

air and water cooled specimens, respectively, than that of hot-press cooled specimen as shown in Fig. 9. The matrix has been torn off and a large amount of fibres had been broken in the hot-press cooled specimen.

Referring to the higher magnification of SEM photos of the fracture surfaces, Figs 12–14, it was found that there was a layer of matrix still adhering to the glass fibres in the hot-press cooled sample as shown in Fig. 12. However, there are clear fibre surfaces appearing in the air and water cooled samples, CII and CIII, Figs 13 and 14, respectively. This verified that the rupture occurred between the glass fibres and the nylon6 matrix (see Figs 13 and 14) in the CII and CIII samples. However, the rupture occurred in the matrix region in the slow cooled GF/PA6 samples. In other words, it means when the interfacial strength is higher than that of the matrix, the rupture occurred in the matrix as shown in the Fig. 12. Otherwise, the rupture occurred between the fibres and matrix when the interface is weaker than the matrix as shown in Figs 13 and 14. Therefore, the flexural strength of the GF/PA6 specimens with fast cooling processes could, in an indirect way, relate to the interfacial bonding strength. However, the flexural tensile strength of the slow cooled GF/PA6 specimens represented the flexural tensile strength of the nylon6 matrix. According to the mechanical test results (Table IV) and the micro-analysis, it can be inferred that increasing cooling rate resulted in a weaker interfacial bond as verified by the SEM photos of the fracture surface of the air and water cooled samples. The fibres surfaces were very clear and there was no evidence of matrix attached to the fibres. The interfacial strength increased with decreasing cooling rates in thermal processes.

From the previous study in the part 1 of the paer [13] of a transmitted polarised light image of the GF/PA6 thin films, we observed columnar spherulites growth along the glass fibre in the hot-press cooled GF/PA6

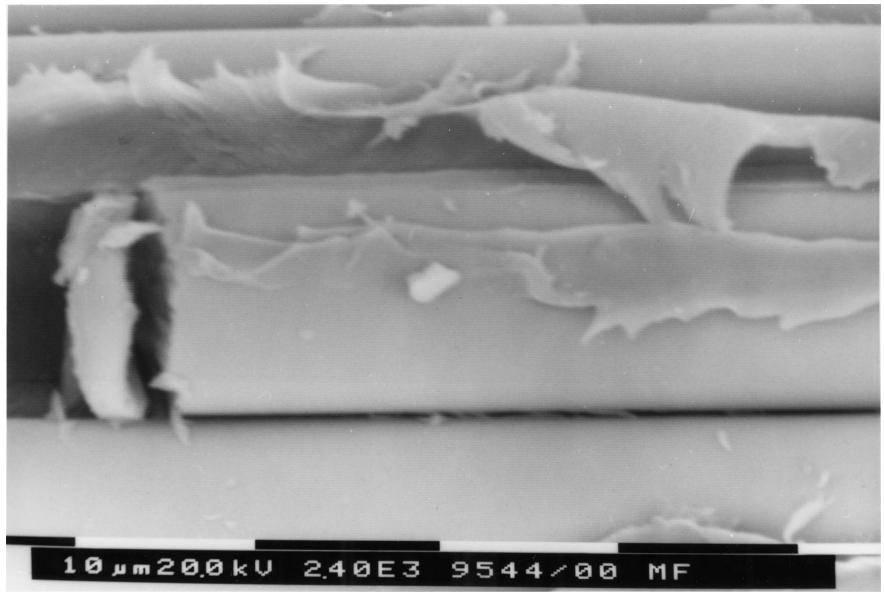

Figure 12 SEM photo of fracture surface of flexural test of hot-press cooled GF/PA6 bulk sample.

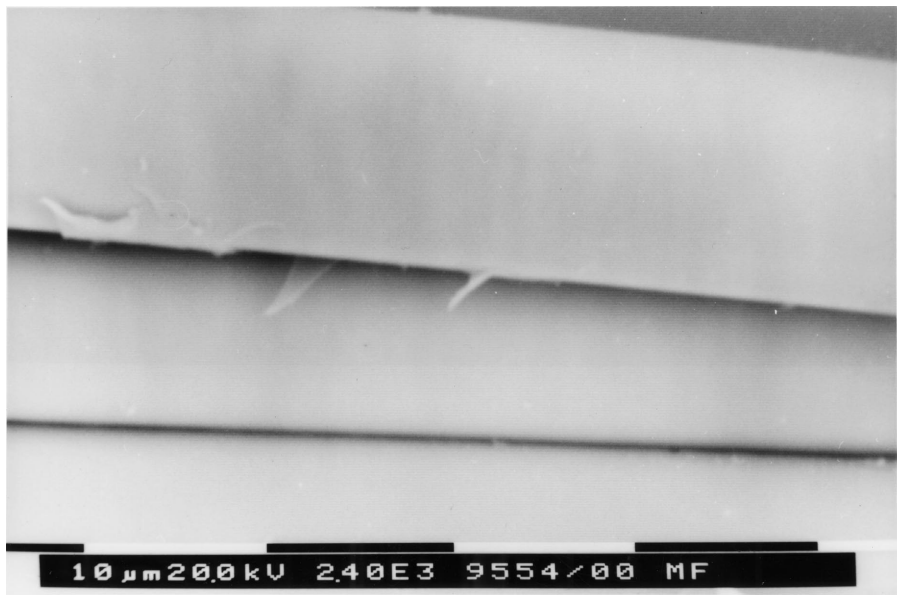

Figure 13 SEM photo of fracture surface of flexural test of air cooled GF/PA6 bulk sample.

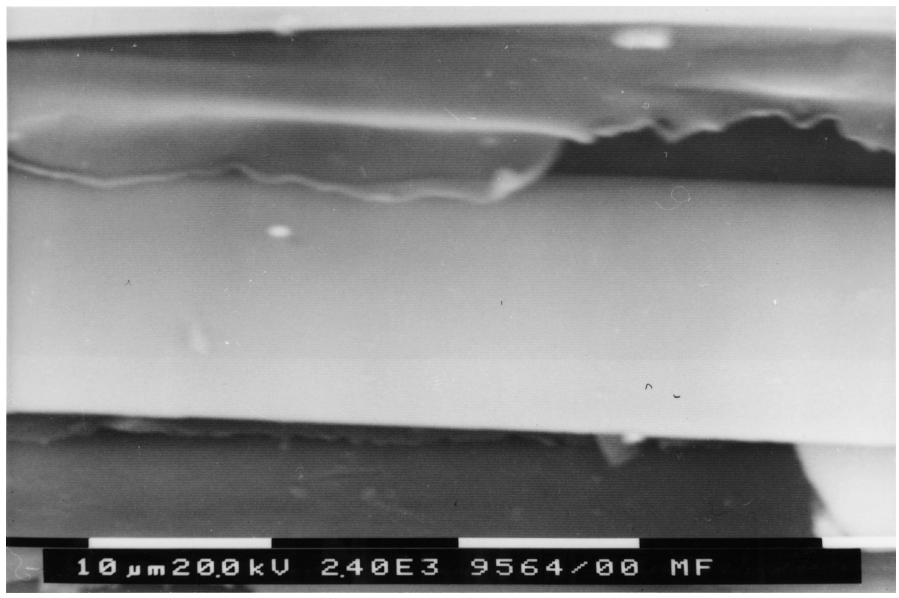

Figure 14 SEM photo of fracture surface of flexural test of water cooled GF/PA6 bulk sample.

sample. The spherulite layer disappeared with increasing the cooling rate in the manufacturing processes. The different crystalline layer between the glass fibre and the nylon6 matrix may be a transcrystalline region. It is possible that this improved the interfacial bonding strength and/or transverse flexural strength in the slow cooled GF/PA6 samples.

5.2.2. Iosipescu intralaminar fracture surfaces

From the stress state analysis of the V-notch root axial splitting section, the stress state at this point was tensile stress as mode I fracture dominated the damage zone. It can be seen in SEM photos (Figs 15 and 17). Fig. 15 shows that the fracture surfaces feature of the axial splitting section were very similar to the flexural fracture surface which was typical mode I fracture (Fig. 9). It has been seen in the both SEM photos taken from flexural and Iosipescu fracture surfaces, that the matrix was torn off from the fibre surface vertically to the fibre axis which means mode I fracture contributed to the damage zones in both the tests. Thus, the first axial splitting stress may give an information about the tensile strength of the interfacial bond of the composites.

Subsequent to the axial splitting, secondary failure and ultimate failure followed with increasing load. The failure modes of the latter (secondary and ultimate) were pure shear failure. It can be verified by the SEM study of the midplane cracking section, Fig. 16. The surface feature shows typical shearing plastic deformation. The matrix was torn off and plastic flow 45° to the fibre axis approximately as shown in Fig. 16. Thus, the secondary failure stress and ultimate failure stress may directly indicate the shear strength of the interfacial bond of the GF/PA6 composites.

The effect of the cooling rate on the interfacial bond can be seen in Figs 17–19 which are the axial splitting fracture surfaces of the three different cooling

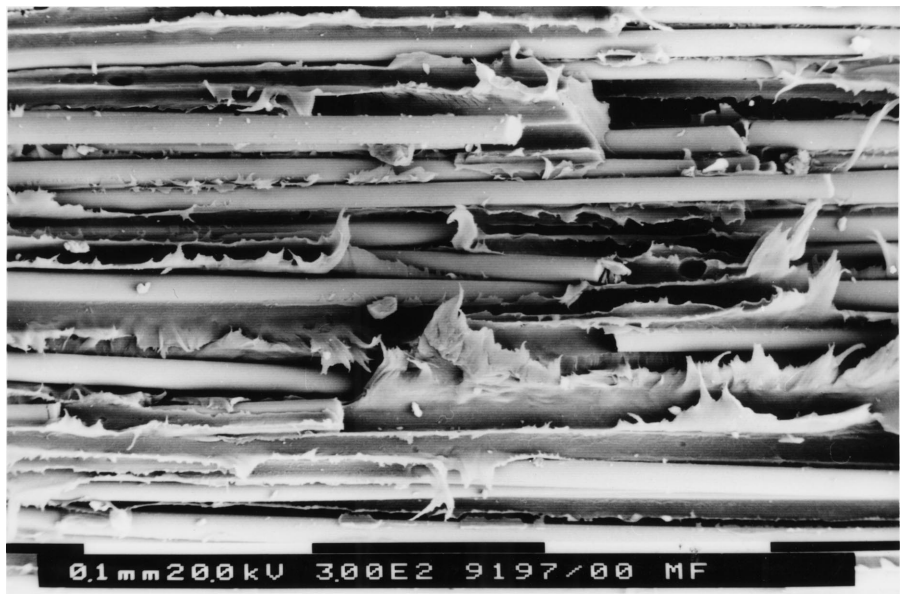

Figure 15 SEM photo of Axial splitting section fracture surface of Iosipescu test.

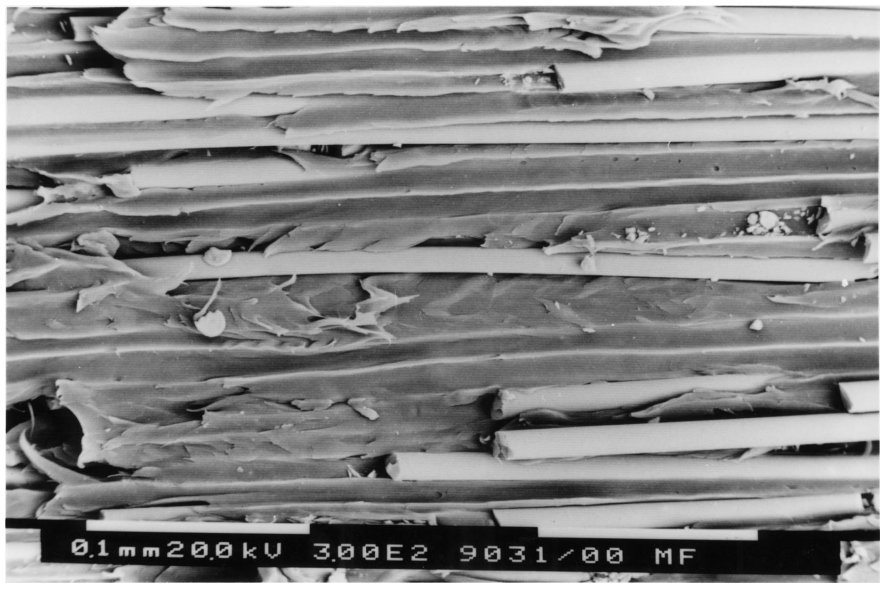

Figure 16 SEM photo of midplane section fracture surface of Iosipescu test.

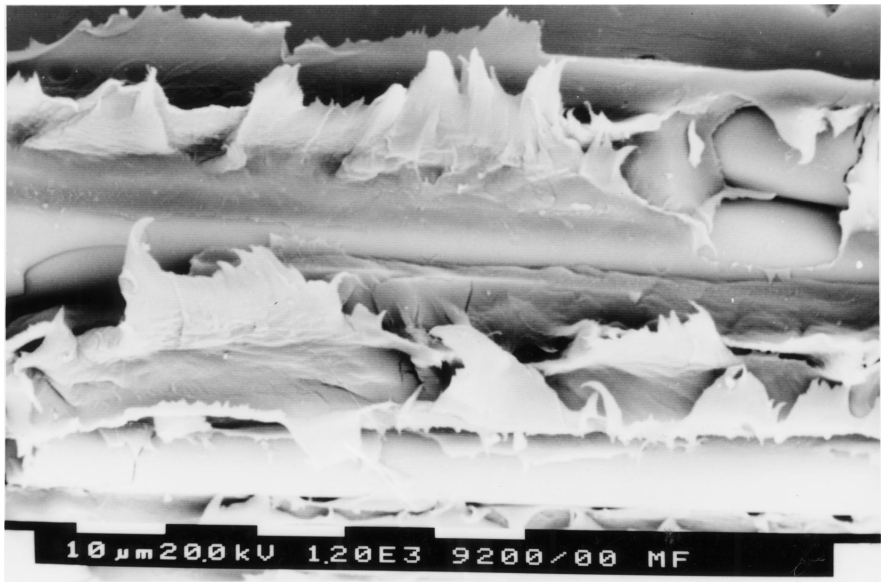

Figure 17 SEM photo of axial splitting section fracture surface of hot-press cooled GF/PA6 sample.

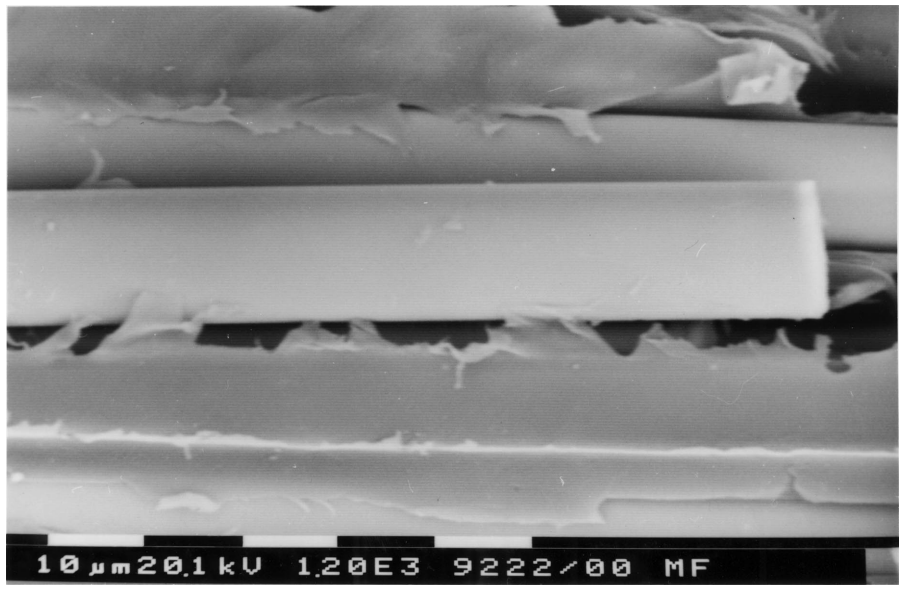

Figure 18 SEM photo of axial splitting section fracture surface of air cooled GF/PA6 sample.

rate specimens. Clearer fibre surfaces appeared in the Figs 18 and 19 which were the air and water cooled specimens, respectively, than that of hot-press cooled specimen as shown in Fig. 17. In Fig. 17, which was the fracture surface of the hot-press cooled specimen, a layer of nylon6 matrix still adhered to the glass fibres in the hot-press cooled sample.

To study the shear fracture mechanisms of the three different cooling samples, a few SEM photos of the fracture surfaces at midplane cracking section have been taken. Fig. 20 shows that a large amount of fibre breakage appeared on the fracture surface of the hot-press cooled sample. The large amount of fibre breakage were caused by shear stresses. The shear stresses were transferred from the matrix to the fibres across the strong interfacial bond which was achieved in the slow cooling process. The strong interfacial bond seemed to prevent the matrix being peeled off and transferred the shear stress to the fibres. However, there was a different situation for the air and water cooled specimen surfaces as shown in Figs 21 and 22. There were long fibres being pulled out by the shear stress and left holes in the matrix. The fibre surface appeared clear. This means the interfacial bond in the fast cooled samples was not good as the slow cooled samples.

From the micro-analysis of the SEM observations, it is verified that the Iosipescu shear strength could, in a direct way, relate to the interfacial shear strength. However, the tensile strength from this test may relate to the interfacial tensile strength indirectly due to the fact that the axial splitting involved both mode I and mode II fractures in this area. The actual stress state was very complex in the axial splitting section area.

It can be concluded that the interfacial strength was higher in the slowly cooled samples than in the fast cooled samples. The slow cooling gave the samples a good interfacial bond and high transcrystallinity, consequently resulted in a high shear strength and tensile

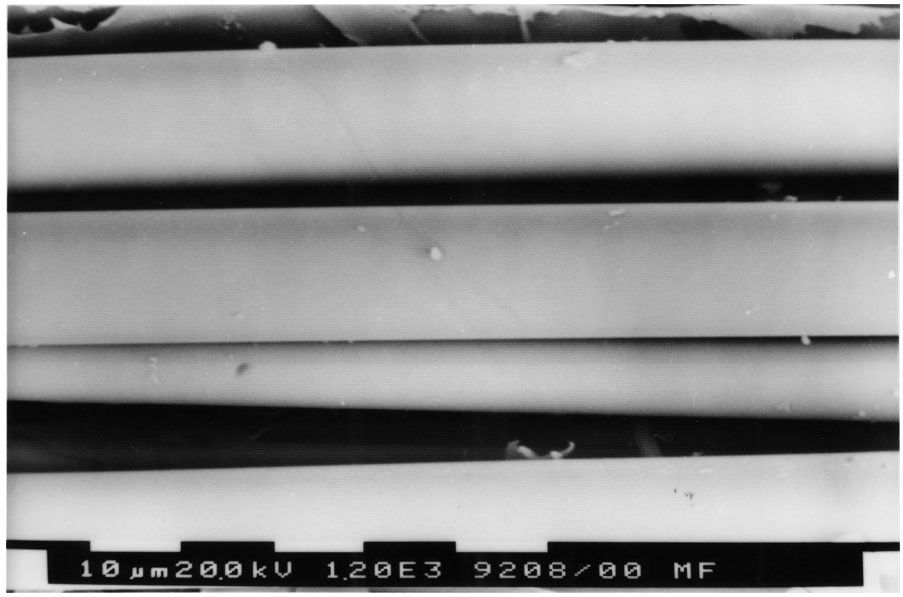

Figure 19 SEM photo of axial splitting section fracture surface of water cooled GF/PA6 sample.

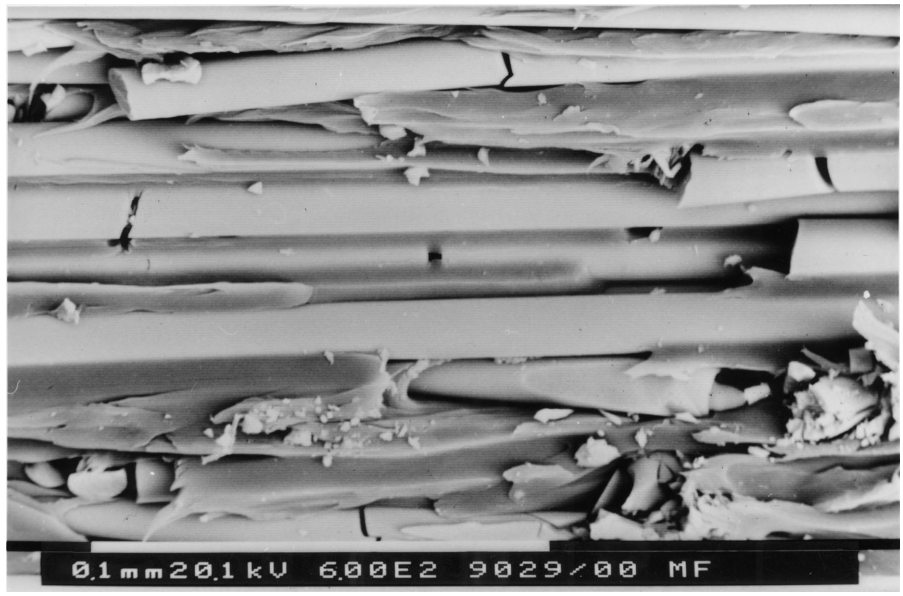

Figure 20 SEM photo of midplane section fracture surface of hot-press cooled GF/PA6.

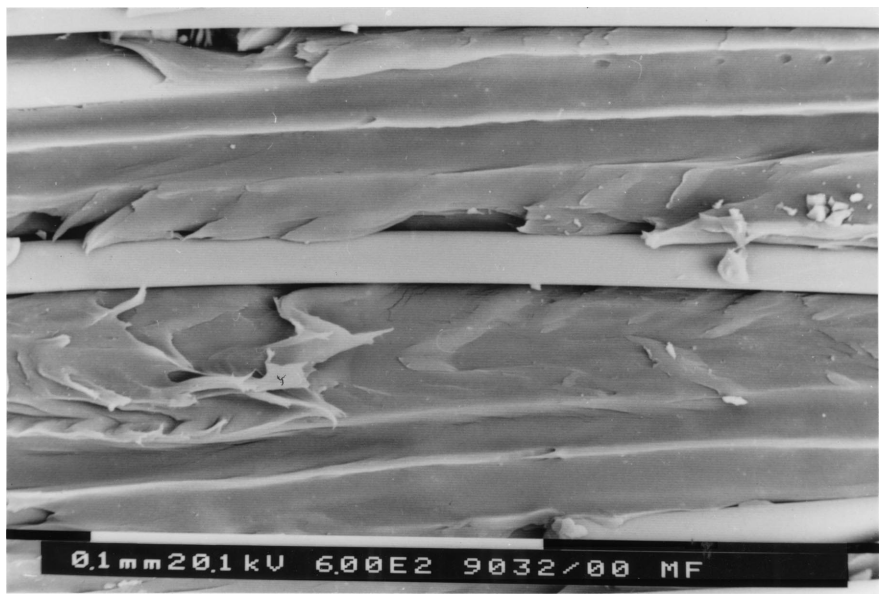

Figure 21 SEM photo of midplane section fracture surface of air cooled GF/PA6.

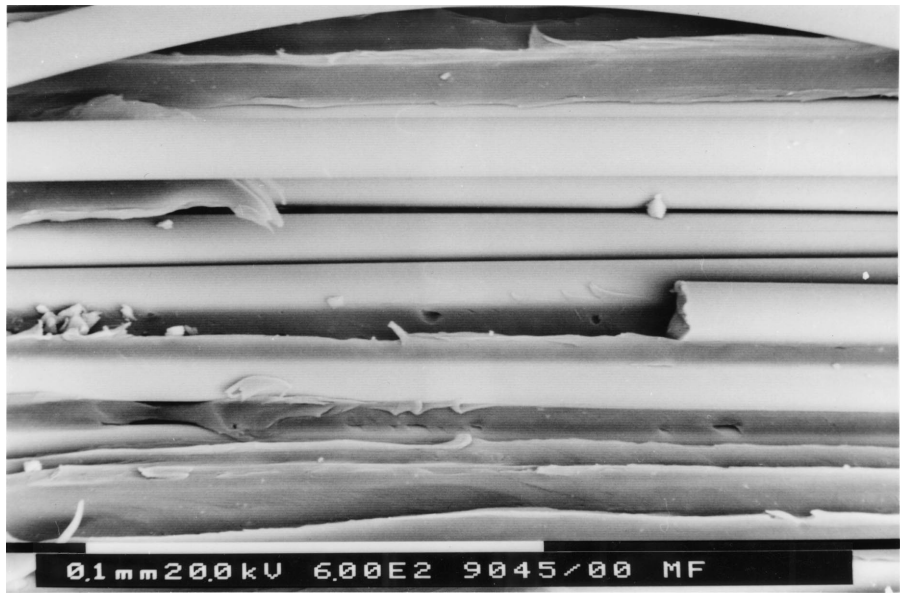

Figure 22 SEM photo of midplane section fracture surface of water cooled GF/PA6.

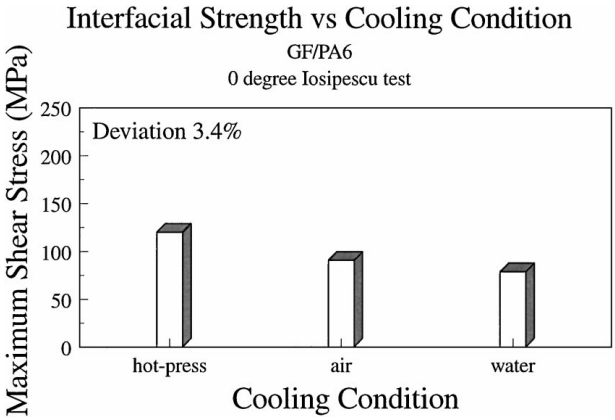

Figure 23 The trend of interfacial shear strength vs cooling condition of 0° GF/PA6 specimen in Iosipescu test.

strength. High crystallinity of the α phase gave the matrix high density contributing to the results as well. The trends of the interfacial shear strength from the Iosipescu tests are shown in Fig. 23.

6. Conclusions

Use of the flexural and Iosipescu tests for investigating the interfacial bond and mechanical properties of the unidirectional GF/PA6 bulk composites in relation to the thermal processing have been conducted experimentally. The failure mechanisms of these tests in relation to the microstructures of the composites were analysed using SEM techniques. The results obtained in this research led to the following conclusions.

(1) Cooling rate during thermal process has significantly affected the mechanical and interfacial properties of the GF/PA6 composites. Slow cooling resulted in a better interfacial bond between the glass fibre and nylon6 matrix than that of fast cooling. It led to a high maximum tensile stress and elastic modulus in the transverse flexural test. These results can be attributed to the high transcrystallinity achieved in the slow cooled GF/PA6 samples. The high crystallinity and high content of the α phase in the slow cooled PA6 matrix contributed to the high tensile strength and elastic modulus in the transverse flexural test as well.

(2) The 0° specimen Iosipescu test results showed that the interfacial shear strength of the slow cooled GF/PA6 was higher than that of fast cooled samples perhaps contributing to its high transcrystallinity.

The results of this paper can be summarised in the table below:

Samples cooling rate (°C/min)	Flexural test σ_{max} (MPa)	Iosipescu test τ_{ult} (MPa)	Flexural test E (GPa)
−1	43	120	4.3
−3	34.5	91	3.5
−60	33	79	2.4

Acknowledgements

The authors would like to give their special thanks to Professor Mike Swain who is from Mechanical and Mechatronic Engineering Department of Sydney University for the many long and valuable discussions through out this study. The authors would also like to acknowledge the Australian Postgraduate Research Award for the financial support given to Dr. Helen Cartledge throughout this study and the Toyobo Research Institute, Japan, for providing the GF/PA6 commingled yarn materials used in this study.

References

1. J. SEFERIS, C. AHLSTROM and S. H. DILLMAN, "Cooling Rate and Annealing as Processing Parameters for Semicrystalline Thermoplastic Based Composites," ANTEC, 1987, pp. 1467–1471.
2. S. SIELLO, J. KENNY and NICOLAIS, *J. Mater. Sci.* **25** (1990) 3493–3496.
3. P. CURTIS, P. DAVIES, I. K. PATRIDGE and J. P. SAINTY, in Proceeding of ICCM6-ECCM2 (Elsevier Applied Science, London, 1987) pp. 4.401–4.412.

4. T. KWEI, H. SCHONHORN and H. L. FRISCH, *J. Appl. Phys.* **38** (1967) 2512.
5. S. MATSUAKA, J. H. DAANE, H. E. BAIR and T. K. KWEI, *J. Polym. Sci. Polym. Lett. Ed.* **6** (1968) 87.
6. M. KANTZ and R. D. CORNELIUSSEN, *ibid.* **11** (1973) 279.
7. D. CAMPBELL and M. M. QAYYUM, *J. Mater. Sci.* **12** (1977) 2427.
8. B. HAISO and E. J. CHEN, in "Controlled Interphases in Composite," edited by H. Ishida (Elsevier Science, New York, 1990) pp. 613–622.
9. J. DENAULT, *Composite Interfaces* **2**(4) (1994) 275–289.
10. F. COGSWELL, in Proceedings of the 28th National SAMPE Symposium, 1983, pp. 528–534.
11. Y. LEE and R. S. PORTER, *Polym Eng Sci* **26** (1986) p. 633.
12. M. HUSON and W. J. MCGILL, *J. Polym. Sci. Polym. Chem. Ed.* **22** (1984) 3571.
13. H. CARTLEDGE and C. A. BAILLIE, *J. Mater. Sci.* **34** (1999) 5099.
14. J. RUSSELL and D. B. CURLISS, in 23rd International SAMPE Technical Conference, October 1991, pp. 91–103.
15. *Idem.*, Journal of Thermoplastic Composite Materials **5** (1992) 238–255.
16. M. FOLKES, G. KALAY and A. ANKARA, *Composites Science and Technology* **46** (1993) 77–83.
17. G. SHONAIKE and M. MASAOU, in International Symposium of Advance Materials, Japan, 1993, pp. 221–225.
18. A. TREGUB, H. HAREL and G. MAROM, *Composites Science and Technology* **48** (1993) 185–190.
19. N. IOSIPESCU, *Studii si Cercetari de Mecanica Aplicata* **13**(3) (1962).
20. *Idem.*, *Journal of Materials* **2**(3) (1967) 537–566.
21. T. PLACE, Private Communication, Aeronutronic Division, Ford Aerospace and Communications Corporation, Newport Beach, CA, 1974.
22. F. MATTHEWS and R. D. RAWLINGS, "Composite Materials: Engineering and Science, Imperial College of Science, Technology and Medicine," (Chapman and Hall, London, 1994).

Received 5 February 1998
and accepted 8 February 1999